High-Resolution Spatio-Temporal Evaluation of Specular and Diffuse Paths in THz MIMO Channels

Seun Sangodoyin, Mine Kerpicci, Chia-Lin Cheng, and Alenka Zajić
Georgia Institute of Technology, Atlanta, GA 30332 USA

***Abstract*—In this paper, we present spatio-temporal analysis of discrete and diffuse multipath components (or paths) present in a propagation channel at Terahertz (THz) frequencies. These paths were extracted using a high-resolution parameter extraction algorithm RIMAX – an iterative maximum likelihood algorithm. For our analysis, we used measurement data obtained from a THz ($300-312$ GHz) 4×4 Multiple-Input-Multiple-Output (MIMO) measurements conducted in an obstructed Line-of-Sight (OLOS) scenario in a data center environment. We provide statistical model for parameters such as mean direction-of-departure (DOD), mean direction-of-arrival (DOA) and the relevant angular and delay spreads. We provided a closed-form model for the diffuse path propagation along with statistical models for relevant spatial and temporal parameters. We showed that diffuse paths contribute a moderate amount of energy (mean value of 12.7%) to the overall energy measured in the THz MIMO Channel. Results in this work is important to wireless system design and development at THz frequencies.**

I. Introduction

Increasing demand for high data rate communication and the need for precision and accuracy in detection, localization and tracking has led to a proliferation of research at Terahertz (THz) frequencies. The THz band is being envisioned for various applications spanning wireless communications to low-proximity ranging. The development of any wireless system catering to the aforementioned applications will require a comprehensive and accurate characterization of the propagation channel in which the system will operate. Hence, It is of utmost importance that such a channel be duly investigated through propagation channel measurements and modeling. The propagation channel can be considered as the superposition of specular and diffuse Multipath Components (MPCs) – with the addition of noise. The development of a comprehensive channel model necessitates the inclusion of spatio-temporal parameters of the discrete and diffuse paths.

Several works such as [1] and [2] have addressed propagation at THz frequencies. Much emphasis has been placed on specular/deterministic components in a propagation channel with the aforementioned works primarily focusing on parameters that can be computed from specular components such as pathloss, shadowing, rms delay spread and small-scale fading factors without consideration for spatial parameters and/or diffuse paths in the propagation channel. To the best of our knowledge, there are no works in which high resolution parameter extraction has been carried out at the THz frequency with consideration for spatial parameters or a closed-form model of the diffuse/dense multipath component (DMC). The novelty of this work is the use of a high resolution iterative maximum likelihood algorithm RIMAX [3] for spatial-temporal parameter extraction at the THz frequency band and the closed-form modeling of dense multipath components in the aforementioned frequency band.

DMC consists mainly of a large amount of weak MPCs birthed as a result of scattering from objects that are either small in size compared to the wavelength of the incident waveform or have rough surfaces. It is usually described as the residual after the specular component in the channel response has been extracted. In scatterer-rich environments, DMCs play a significant role in terms of their contribution to the amount signal power received [3]. The concept of diffuse scattering at THz frequencies has been discussed in [4] and [5], however, there were no closed-form spatio-temporal models for DMC presented in these works. Such a model is particularly important at THz frequencies due to its small wavelengths which renders otherwise "smooth" surfaces rough and produces diffuse components.

In this paper, we provide a spatio-temporal analysis of specular and diffuse components at THz frequencies using empirical data from a 4×4 Multiple-Input-Multiple-Output (MIMO) measurement campaign conducted in an obstructed Line-of-Sight (OLOS) scenario in a data center environment. We provide a statistical model for the aforementioned parameters while also introducing a closed-form model for the dense multipath conponents . The DMC model was validated using a Power-Angular-Delay-Profile (PADP) generated with the extracted model parameters.

The rest of this paper is organized as follows. The description of the measurement conducted is provided in Section II. The system model used in this work is provided in Section III while the results are provided in Section IV. Summary and conclusion are inferred in Section V.

II. Experiment Description

The measurement campaign was conducted in a data center at the Tech Way Building on the campus of the Georgia Institute of Technology. At the heart of our channel sounder is a Vector Network Analyzer (VNA) Keysight N5224A PNA. This is a two-port device, which provided the complex frequency response of the propagation channel. The stepped frequency sweep on the VNA transversed 801 frequency points with a bandwidth of 12 GHz. The VNA was connected to Virginia Diode Inc (VDI) up and down transceivers for frequency modulation (and demodulation) to (and from) the

300 – 312 GHz band. A 24 dBi vertical polarized horn antenna with a 3 dB beamwidth of 10° was used at the transmitter (Tx) and receiver (Rx) ends in our measurement setup. These antennas were arrange such that a 4×4 Multiple-Input-Multiple-Ouput (MIMO) virtual Uniform Linear Array (ULA) configuration was constructed using a 1 mm antenna separation distance with the Tx and Rx positioned at a 0.15 m Line-of-Sight (LOS) Euclidean displacement. To simulate a possible impediment to propagation in a data center, we conducted propagation measurements in an obstructed Line-of-Sight (OLOS) scenario with cables (power and auxiliary functional) serving as obstruction in the propagation path of the wireless signal. It is noteworthy that since THz signals are best suited for low-proximity point-to-point communication, the presence of an impediment in the propagation path would be of significant consequence to the fidelity of the received signal. To this end, we used 5 OLOS channel realization – with each realization corresponding to varying obstructing cable thickness. An illustration of the aforementioned scenario has been provided in Fig. 1 while a depiction of Tx and Rx arrangements in the data center has been provided in Fig. 2. It is important to note that the Tx and Rx have been placed in racks housing the data servers in this environment. The expected interacting objects and reflectors – in addition to the obstructing cables – is comprised of by metal structures of the server racks. An extensive discussion on the measurement campaign carried out in this environment has been provided in [2].

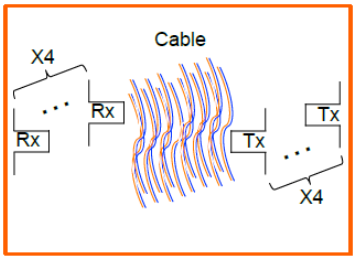

Fig. 1: Illustration of the cable obstruction in the LOS THz MIMO Channel.

The channel sounder provides a 3-dimensional transfer function matrix $\mathbf{h}(f,t,r) \in \mathbb{C}^{M_{\mathrm{T}}\times M_{\mathrm{R}}\times M_f}$ with variable f corresponding to the measured frequency index while $t \in M_{\mathrm{T}}$ and $r \in M_{\mathrm{R}}$ represent the TX and RX antenna elements respectively.

III. System Model

In this work, the wireless propagation channel ($\mathbf{h}$) will be modeled as a superposition of specular/deterministic paths ($\mathbf{S}(\theta_{\mathrm{sp}})$), dense multipath components (DMC, $\mathbf{D}(\theta_{\mathrm{dmc}})$) and measurement noise ($\mathbf{n}$):

$$\mathbf{h} = \mathbf{S}(\theta_{\mathrm{sp}}) + \mathbf{D}(\theta_{\mathrm{dmc}}) + \mathbf{n} \quad \in \quad \mathbb{C}^{M_{\mathrm{T}}M_{\mathrm{R}}M_f\times 1}. \tag{1}$$

Specular paths represents the set of plane waves in the environment, while the DMC can be explained by diffuse

Fig. 2: Measurement setup in the LOS THz MIMO Channel.

scattering. A specular component $\mathbf{S}(\theta_{\mathrm{sp}})$ can be characterized by its parameter θ_{sp}, which contains the time-delay τ, azimuth angle-of-arrival φ_{Rx}, azimuth angle-of-departure φ_{Tx} and the complex amplitude/path-weight Γ such that the specular component obtained with a superposition over an ensemble of L paths in the propagation channel can be modeled as

$$\mathbf{S}(\theta_{sc}) = \sum_{l=1}^{L} \mathbf{B}_{\mathrm{R}}^{T}(\varphi_{R,l}) \cdot \Gamma_l \cdot \mathbf{B}_{\mathrm{T}}(\varphi_{T,l}) \cdot e^{-j2\pi f \tau_l} \tag{2}$$

where $\mathbf{B}_{\mathrm{R}}(\varphi_{R,l})$, $\mathbf{B}_{\mathrm{T}}(\varphi_{T,l})$ denote the antenna array beampattern responses to the azimuth angles of arrival and departure for the l-th path with Γ_l representing the complex path weight and τ_l is the time-delay of the l-th path, respectively. For the temporal and spatial analysis relevant to this work, the high resolution parameter estimation framework RIMAX [3] was used for the extraction of the aforestated parameters so as to produce an antenna independent characterization of the radio channel.

The DMC, which describes the stochastic part of the propagation channel, is assumed to comprise of a large number of individually weak signal components that cannot be estimated individually as plane waves, e.g., because of the underlying physical process (diffuse scattering, wavefront curvature, etc.). Therefore, owing to the central limit theorem, $\mathbf{D}$ (to simplify our notation, we will denote $\mathbf{D}(\theta_{\mathrm{dmc}})$ as $\mathbf{D}$ henceforth) is modeled as a zero-mean complex circularly symmetric Gaussian distributed random vector with a covariance matrix $\mathbf{R}_{\mathrm{D}} \in \mathbb{C}^{M_{\mathrm{T}}M_{\mathrm{R}}M_f\times M_{\mathrm{T}}M_{\mathrm{R}}M_f}$, i.e., $\mathbf{D} \sim \mathcal{N}_c(0,\mathbf{R}_{\mathrm{D}})$. The measurement noise is assumed to be a white complex circularly symmetric Gaussian distributed random vector $\mathbf{n} \sim \mathcal{N}_c(\mathbf{0},\sigma_{\mathrm{N}}^2\mathbb{I})$ with variance σ_{N}^2. The DMC is described by its covariance matrix $\mathbf{R}_{\mathrm{D}}$ and can be decomposed into the Kronecker-product of three matrices [3]:

$$\mathbf{R}_{\mathrm{D}} = \mathbf{R}_{\mathrm{R}} \otimes \mathbf{R}_{\mathrm{T}} \otimes \mathbf{R}_{\mathrm{F}}, \tag{3}$$

where $\mathbf{R}_{\mathrm{F}}$ is the covariance matrix in the frequency domain while $\mathbf{R}_{\mathrm{R}}$ and $\mathbf{R}_{\mathrm{T}}$ are the covariance matrices of the antenna array elements at the Tx and Rx. The frequency domain covariance matrices can be modeled by $\mathbf{R}_{\mathrm{F}} = \mathrm{toep}(\bar{\lambda}(\theta_{\mathrm{F}}), \bar{\lambda}(\theta_{\mathrm{F}})^{\dagger})$, where the operator $\mathrm{toep}(\cdot)$ denotes a Toeplitz matrix and $\bar{\lambda}$ is

a sampled version of the power spectral density, given by

$$\bar{\lambda}(\theta_{\mathrm{F}}) = \frac{\tilde{\alpha}_1}{M_f}\left[\frac{1}{\tilde{\beta}_{\mathrm{d}}}, \frac{e^{-j2\pi\tau_{\mathrm{d}}}}{\tilde{\beta}_{\mathrm{d}} + j2\pi\frac{1}{M_f}}, \cdots, \frac{e^{-j2\pi(M_f-1)\tau_{\mathrm{d}}}}{\tilde{\beta}_{\mathrm{d}} + j2\pi\frac{M_f-1}{M_f}}\right]^T. \quad (4)$$

The parameters of the frequency domain (or time-domain equivalence) covariance matrix model are $\theta_{\mathrm{F}} = [\tau_{\mathrm{d}},\ \tilde{\beta}_{\mathrm{d}},\ \tilde{\alpha}_1]^T$, where β_{d} is the normalized coherence bandwidth of the channel, τ_{d} and $\tilde{\alpha}_1$ are the delay of arrival and power of the first component in the time domain equivalent (i.e., inverse Fourier transform) of $\mathbf{R}_{\mathrm{F}}$.

In a multi-antenna setup, the spatial covariance matrices ($\mathbf{R}_{\mathrm{T}}$ and $\mathbf{R}_{\mathrm{R}}$) can be modeled as:

$$\mathbf{R}_{\mathrm{R/T}} = \mathbf{B}_{\mathrm{R/T}} \cdot \mathbf{K}(\theta_{\mathrm{R/T}}) \cdot \mathbf{B}^{\dagger}_{\mathrm{R/T}}, \quad (5)$$

where $\mathbf{B}_{\mathrm{R/T}}$ denotes the antenna array responses at Rx and Tx, while $\mathbf{K}(\theta_{\mathrm{R/T}})$ is a diagonal matrix whose entries are determined by the angular probability density distribution of the DMC, which is modeled as Von-Mises Distribution (VMD) with a Uniform Distribution (UD) extension thereby resulting in a PDF defined as:

$$f_{\mathrm{VMD,\ UD}}(\varphi, \mu, \kappa, \bar{\alpha}) = e^{\kappa\ \cdot\ cos(\varphi-\mu)} \cdot e^{-\kappa}\left(\hat{A} - \bar{\alpha}\right) + \bar{\alpha}, \quad (6)$$

where μ is the mean angle, κ is the concentration parameter, $\bar{\alpha}$ is the amplitude of the additional uniform distribution and $\hat{A}$ is a normalization factor. Parameters of $\mathbf{K}(\theta_{\mathrm{T/R}})$ in the spatial domain are given by $\theta_{\mathrm{T}} = [\mu_{\mathrm{TX}}, \kappa_{\mathrm{TX}}, \bar{\alpha}_{\mathrm{TX}}]$ and $\theta_{\mathrm{R}} = [\mu_{\mathrm{RX}}, \kappa_{\mathrm{RX}}, \bar{\alpha}_{\mathrm{RX}}]$, respectively.

IV. Results

A. Specular Component Analysis

The statistical estimates, relevant distribution fits and correlation between the extracted specular parameters will be subsequently discussed.

*1) **Statistical Model Parameters of Specular Components**:* We computed the first and second moments from the extracted parameters to obtain the mean Direction-of-Departure (DOD) and mean Direction-of-Arrival (DOA) and their corresponding spreads i.e. Azimuth-spread-of-Departure (ASD) and Azimuth-spread-of-Arrival (ASA). We also computed the Root-Mean-Squared (RMS) delay spread of the extracted paths. A statistical distribution fit of these parameters revealed that the mean DOD and DOA follow a Gaussian distribution while the angular and delay spread parameters are lognormally distributed. The first and second moments of these parameters have been provided in Table I while the empirical Cumulative distribution function (CDF) and corresponding distribution fits of the angular spreads are shown in Figs. 3(a) - 3(b).

It can observed from the results presented in Table I that the mean AOD and mean AOA are close to zero i.e., in the LOS orientation. This is understandable given that the measurement was actually designed for a LOS scenario with the introduction of cables to act as propagation impediments/blockages. These results inform that strong LOS paths were still permissible in the channel even with the obstructing cables i.e., we did not experience a total occlusion of the LOS signal. The slightly large spread also informs on the impact of reflectors and scatterers in the vicinity of both the Tx and Rx.

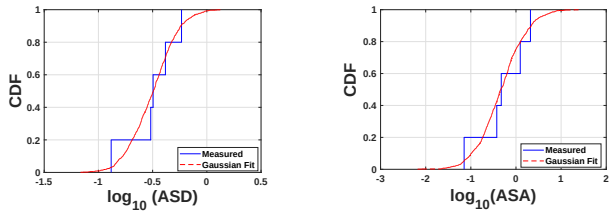

(a) (b)

Fig. 3: CDF of (a) $\log_{10}(\mathrm{ASD})$ and (b) $\log_{10}(\mathrm{ASA})$

TABLE I: Parameters of distr. fits of specular components

Parameter	Mean	Std. Dev.
Mean AOD (°)	0.10	0.12
Mean AOA (°)	0.04	0.22
ASD (dB)	−0.29	0.51
ASA (dB)	−0.50	0.22
τ_{rms} (dBns)	−9.41	0.23

Moments of ASD, ASA and τ_{rms} were computed as $\log_{10}(\cdot)$.

*2) **Correlation of Spatio-Temporal Parameters**:* The correlation between spatial and temporal parameters was also explored in this work with a graphical depiction of the correlation coefficient provided in Fig. 4.

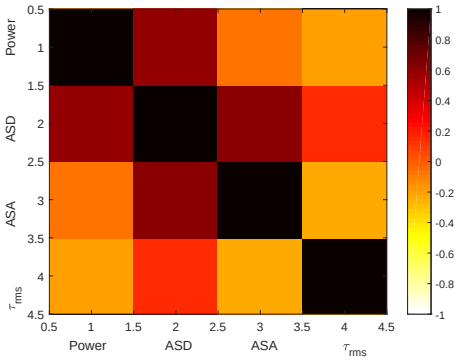

Fig. 4: Correlation coefficient matrix of specular parameters.

It can be observed from Fig. 4 that while parameters such as ASD and ASA are positively correlated, other parameters such as power and τ_{rms} show a negative correlation – an intuitively understandable observation.

B. Dense Multipath Component Analysis

DMC spatial-temporal parameters were extracted at the various channel realizations in our work. Statistical distribution fits and corresponding moments for the extracted parameters are provided in Table II while sample plot of the CDF for parameters such as α_1 confirms a good-fit of its logarithmic equivalent to the Gaussian distribution as shown in Fig. 6. To ascertain our proposed approach to modeling the dense multipath components in the THz MIMO channel, we synthesized

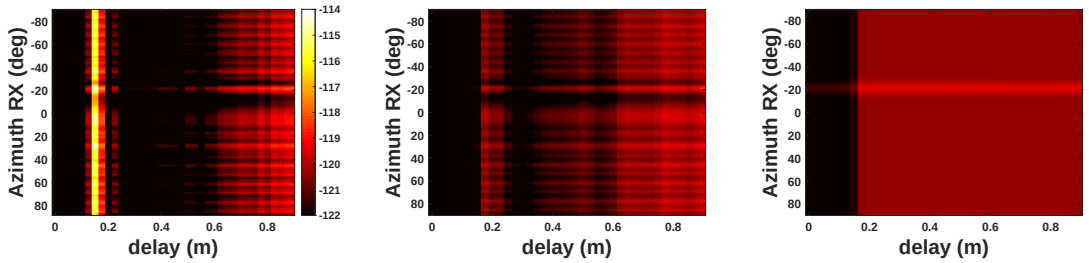

(a) Measured total (b) Residual (c) Modeled residual

Fig. 5: PADP comparison at the RX from (a) measured channel, $\mathbf{h}$ (b) residual channel, $\mathbf{h} - (\mathbf{S}(\theta_{\text{sp}}))$ and (c) modeled DMC.

the DMC by using eqs. (3) to (6) and generated the PADP of the measurement data, which includes both specular and residual (i.e. DMC) components, extracted residual components only (from the measurement data) and the modeled residual at the Rx end. The plots for the PADP are shown in Figs. 5(a) to 5(c). It can be clearly observed from the aforementioned figures that the modeled residual does fit well to the residual obtained from the actual measurement data.

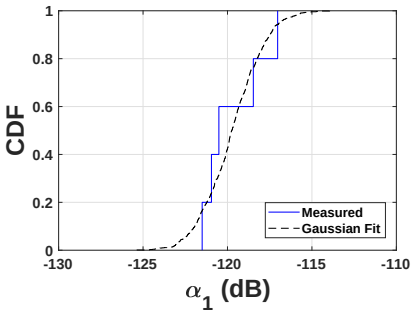

Fig. 6: CDF of DMC parameter α_1 (dB) with Gaussian fit.

TABLE II: DMC parameters and corresponding distr. fit

Parameter	Mean	Std. Dev.	Distribution
rel. $\mu_{\text{TX}}(^\circ)$	5.35	8.53	Gaussian
rel. $\mu_{\text{RX}}(^\circ)$	4.75	7.77	Gaussian
α_1 (dB)	-119.69	1.68	Gaussian
κ_{TX} (dB)	22.98	0.82	Lognormal
κ_{RX} (dB)	22.98	0.82	Lognormal
β_d	0.01	0.01	Gaussian
τ_d (dBns)	-92.70	0.12	Lognormal
$\bar{\alpha}_{\text{TX}}$	8.76×10^{-5}	1.69×10^{-5}	Gaussian
$\bar{\alpha}_{\text{RX}}$	9.25×10^{-5}	2.98×10^{-5}	Gaussian

Note that rel. $\mu_{\text{TX/RX}}$ correspond to the angular orientation relative to the geometric LOS.

The amount of power that the DMC ($\hat{\eta}_{\text{dmc}}$) contributes to the total channel power is calculated from the $\mathbf{R}_{\text{D}}$ (see (7)). The DMC power ($\hat{\eta}_{\text{dmc}}$) can be computed as:

$$\hat{\eta}_{\text{dmc}} = \text{Tr}\{\mathbf{R}_{\text{D}}\} \tag{7}$$

where $\text{Tr}(\cdot)$ is the *Trace* of a matrix. The fractional DMC power is expressed as $f_{\text{dmc}} = \frac{\hat{\eta}_{\text{dmc}}}{P_{\text{Tot}}} \cdot 100\%$, i.e., the percentage the DMC contributes to the total channel power (P_{Tot}). The CDF of f_{dmc} computed in this work has been provided below in Fig. 7.

The average value for f_{dmc} is 12.7%, which implies that the power contribution of the DMC can be considered as moderate for this measurement campaign.

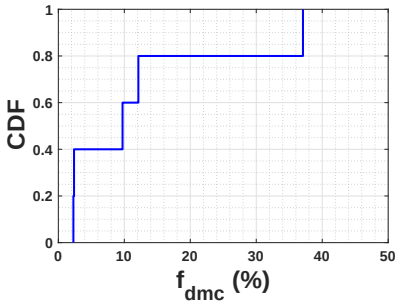

Fig. 7: CDF of the fractional DMC

V. Summary and Conclusion

We succeeded in extracting parameters from a THz MIMO channel using a high resolution parameter estimation algorithm RIMAX. The spatio-temporal parameter spreads at both Tx and Rx ends were found to be lognormally distributed. We modeled and validate the diffuse paths in the propagation channel and also found that the diffuse paths contribute a moderate amount of energy (mean value of 12.7%) to the overall energy measured in the THz MIMO Channel.

References

[1] J. M. Eckhardt, T. Doeker, S. Rey, and T. Krner, "Measurements in a real data centre at 300 ghz and recent results," in *2019 13th European Conference on Antennas and Propagation (EuCAP)*, 2019, pp. 1–5.

[2] C. Cheng, S. Sangodoyin, and A. Zaji, "Terahertz MIMO Fading Analysis and Doppler Modeling in a Data Center Environment," in *2020 14th European Conference on Antennas and Propagation (EuCAP)*, 2020, pp. 1–5.

[3] A. Richter, "Estimation of radio channel parameters: Models and algorithms," Ph. D. dissertation, Technische Universität Ilmenau, Ilmenau, Germany, 2005. [Online]. Available: www.db-thueringen.de

[4] C. Jansen, S. Priebe, C. Moller, M. Jacob, H. Dierke, M. Koch, and T. Kurner, "Diffuse scattering from rough surfaces in thz communication channels," *IEEE Transactions on Terahertz Science and Technology*, vol. 1, no. 2, pp. 462–472, 2011.

[5] F. Sheikh, D. Lessy, M. Alissa, and T. Kaiser, "A comparison study of non-specular diffuse scattering models at terahertz frequencies," in *2018 First International Workshop on Mobile Terahertz Systems (IWMTS)*. IEEE, 2018, pp. 1–6.